Research Article

Journal of Nuclear Technology in Applied Science
Year 2024, Volume-12, Issue-1&2 (January - December)

www.acspublisher.com

Theoretical and Experimental Investigation of Two-Phase Sub-Cooled Heat-Pipe at Different Regimes

Elsayed, M.[1], Abd El Badie, A.[1]; Mansour, M. S.[1&2]; Abdel-Raouf, M. M.[1] and Eid, M.A.[1]

[1] Mechanical Engineering Depart. Higher Technological Institute (HTI), Tenth of Ramadan City 44629, Egypt
[2] Mechanical Engineering Depart, Faculty of Engineering. City University of Cairo (CUC), New Heliopolis City, Cairo, Egypt.

ARTICLE INFO

Keywords: *Heat-pipe, Subcooled, Heat Pipe Simulation, transient, Steady-state.*

ABSTRACT

The development of novel sub-cooled two-phase thermosyphon or heat-pipe devices is crucial for improving heat transfer efficiency. The characteristics are looked at using both theoretical models and data from the sub-cooled heat loop that was collected during its steady-state, heating-up, and cooling-down stages. In the heating-up, steady-state, and cooling-down modes, the sub-cooled heat pipe's evaporator length, cooling rate, and effectiveness of the heating rate are experimentally investigated. Several applications, such as the current practical inquiry's irregular operation, rely on the dynamic model of the sub-cooled heat pipe. The study's overarching goal is to provide a theoretical basis for modeling the double-tube evaporator's dynamic properties. The analysis of various transient parameters will be carried out during the warm-up, steady-state, and cool-down phases of operation to achieve this goal. The model faithfully reproduces the temperature and phase properties of a sealed, sub-cooled heat pipe with two distinct phases. A thermal evaporator wall and a working fluid are used in the practical arrangement, and the experimental results show a simple exponential pattern. The theoretical model and the experimental data are highly congruent.

Introduction and methodology

Heat-pipe technology has been implemented in numerous industries to enhance the heat transfer of heat sinks that are based on heat pipes in micro-level electronic engineering. Heating pipelines are appropriate for thermal management in electronics due to the compactness of highly integrated components. The working fluid and electronic circuit can be electrically insulated, and heat-producing and heat-removing elements can be separated in the absence of power. HVAC systems, spacecraft, human bodies, and nuclear reactor technology have all employed conventional heat pipelines as cooling devices **(Kang *et al.*, 2023)**. A recent study has investigated the standard heat pipelines that are employed in solar energy and thermal management

*Corresponding author.
E-mail address: Mohamed.elsayed@hti.edu.eg
Received: 15/10/2024 Accepted: 8/12/2024

systems for electric vehicle batteries **(Weragoda *et al*., 2023)**. The heat transfer of electronic components in satellites, spacecraft, and mechanical systems with ground heat sources has been managed using high-performance heat pipelines **(Zhang *et al*., 2022; Patel, 2018; Li *et al*., 2023)**. Important uses for sub-cooled heat pipes include geothermal systems and nuclear reactor safety systems. From ambient startup conditions to steady-state settings, it keeps the temperature from getting too high by ensuring it stays within prescribed parameters **(Li *et al*., 2023; Yuan *et al*., 2020)**. The original idea of heat pipelines was put out by **Calvin (1992)).** Extensive literature has examined the theoretical and experimental aspects of heat pipe characteristics **(Zhixing *et al*. (2021); Zeqin *et al*. (2021); Xianping *et al*. (2016)). Wang *et al*. (2010)** examined the unstable initiation technique of a cylindrical micro-fluted heat pipe and found that CuO nanofluid can minimize the initiation time. **Zhang *et al*. (2009)** an empirical study was carried out to assess the characteristics of heat transfer by evaporation in an ammonia-filled heat pipe with trapezoidal grooves. In the transient phase, **Parand *et al*. (2009)** used the transient lumped model to theoretically investigate the thermosyphon heat pipe. The analytical formulation for the system's thermal behavior has been developed. **Dobson *et al*. (2007)** used a closed loop thermosyphon was looked at to find out how it works and how much heat it can transfer in order to cool the nuclear reactor cavities in Pebble Bed Modular Reactor (PBMR) applications. Experimental and theoretical studies centered on the initial and transient behavior of the thermosyphon-based PBMR cooling system. The study was conducted by **Dobson *et al*. (2007)**. At various sink temperatures, **Chen *et al*. (2006)** conducted an array of experiments utilizing a miniature loop heat pipe (MLHP) to chill consumer electronics in both the horizontal and vertical orientations. Temperature fluctuations were observed to be highest in the condenser and lowest in the evaporator. The modes of operation of the MLHP were significantly impacted by their orientations. **Jaroslow *et al*. (2006)** calculated the effective heat pipe-conductivity in a transient state through measurements and modeling of mass and heat transfer. The model incorporates the consequences of condensation and liquid evaporation occurring within the heat-pipe. **Kamel *et al*. (2006)** conducted an experimental study to determine how changing the dimensions of the annulus spacing affects the characteristics of the hot fluid channel and the overall efficiency of a closed water-copper two-phase double-tube heat pipe (CTP-DTT). The heat pipe was operated vertically and under steady conditions. The researchers utilized a variety of measurement techniques and resources. **Zeghari *et al*. (2023)** investigated the length of the condensation section, as well as the operating temperature and heat resistance. It was determined that the capacity of the heat pipes was diminished as a result of the condensation portion being reduced. The condensation section may be 60% of the heat pipe's length after the operating temperature is reduced from 90°C to 60°C, as opposed to 40%. In their study, **Imura *et al*. (2005)** initiated a start-up experiment in a two-phase heat-pipe that was frozen. They utilized ethylene glycol aqueous solutions (binary mixtures) at 1% and 2% in conjunction with water working fluid.

Pressure, temperature, heat transfer rate, and mass flow rate should all be considered. **Hua *et al*. (2004)** recorded the characteristics of a semi-open, two-phase heat pipe (SOTPT). In order to gain a comprehensive comprehension of the properties of a SOTPT, its behaviors during ON, OFF, and an absence of water were analyzed. **Saadawy *et al*. (2004)** conducted an experimental investigation into heat transmission in a closed two-phase heat-pipe utilizing a double-tube evaporator. A comparative analysis was performed between this heat pipe and the conventional one. The experimental findings demonstrated that the closed two-phase heat pipe equipped with a double evaporator tube exhibited performance advantages over its conventional counterpart. Experimentally and theoretically, **Saadawy *et al*. (2004)** assembled a closed two-phase double-tube heat-pipe with narrow channels to examine the thermal properties of boiling heat transmission. The performance of the thermal hydraulics of fluid rising in a circulation within a narrow-heated channel was studied in terms of saturated and sub-cooled boiling. The efficient lengths of the non-boiling zones and boiling zones could be deduced from the local distribution of the liquid and wall at axial temperature. The transient regime behavior of TPCTs was investigated experimentally and theoretically by **Farsi *et al*. (2003).** The experiment revealed that there are two types of TPCT responses: one type is for changes that occur consistently and monotonically in the operating system variables, and the other type is for changes in temperature. **Hussein (2002)** examined a two-phase closed heat-pipe with a solar heater by theoretical natural circulation in real-world field settings. The results suggest that there is a statistically significant relationship between the tank's dimensions and both the collector's area and the heater's effectiveness. An analytical model was devised by **Wang *et al*. (2000)** to forecast the performance of a flat plate with a heat-pipe under various practical operation scenarios, including cyclic startup and termination. The transient heat pipe extended "network" model was analyzed by **ZUO *et al*. (1998).** To evaluate the analyses, experimental and theoretical results from the literature were consulted. A dynamic mathematical model for a high-performance heat-pipe with a tube separator with natural circulation and two-phase flow was investigated by **Lin *et al*. (1998)** using a FORTRAN code that described ordinary differential equation systems. A model of a two-dimensional heat-pipe was introduced by **Harley**

***et al.* (1994).** This model incorporates the simultaneous transport of heat in condensate film. A Nusselt-type was used to solve comprehensive transient conservation equations in two dimensions: the loop wall and vapor flow. To verify the model's accuracy, they compared it to previously obtained experimental data. Experimentally, **Huang *et al.* (1993)** examined the kinetic response of an inclined thermosyphon heat pipe to abrupt variations in input power and fluctuating cooling rates. Observed the kinetic response of an inclined thermosyphon heat pipe under abrupt variations in input power and fluctuating cooling rates. The results indicated that increasing the cooling water flow rate to 10 g/s decreased the heat pipe's response time constant. As the water flow rate increases, the magnitude of the variation in the heat pipe time constants diminishes noticeably. **Kwon *et al.* (2023)** investigated the enhancement of thermal performance by minimizing hydrodynamic resistance in heat pipes to accelerate operational fluid flow. A liquid bypass line was constructed. The acceleration of the working fluid was measured in both bypass mode (with all bypass valves open) and regular mode. The experimental results indicated that the heat transfer efficiency of the heat pipe system improved by 106.5% in relation to thermal resistance. The maximum horizontal thermal load rose by 45.8% in bypass mode. **El-Genk *et al.* (1993)** experimentally conducted the water heat-pipe comprises a condenser section that is cooled through convection and an evaporator section that is uniformly heated. The time constants for the temperature of the vapor and the rate at which power is moved during the heating and cooling phases were determined based on the rate at which cooling water flows and the quantity of electric power being supplied. A thorough model was created by **Reed *et al.* (1987).** To forecast the extended and immediate performance of a two-phase closed heat-pipe. To control the shear stress and heat transfer coefficients, these equations were derived by utilizing existing correlations and equations that describe mass, energy balances, and momentum. **Ramos *et al.* (1986)** examined the closed two-phase heat-pipe stability model, considering various factors such as heat input, liquid loading, Grashof's two-phase flow, capillary number, and viscosity. **Liu *et al.* (2023)** created a transient 3D CFD model to study heat pipe liquid–vapor flow and heat transmission. However, such models are computationally demanding and only suitable for stable state calculations or short-term transients.

Continuous operation of the heat pipe is unaffected by the length of the pipe or the ratio of vapor-to-liquid viscosity, according to the researchers. However, the density ratio of the liquid and vapor phases does play a major role. While most heat pipes use a pool boiling mechanism for their evaporation section, heat pipes with a double tube evaporator take a different approach and think about a flow boiling mechanism within. The study aims to look into the flow boiling that is caused by natural circulation in the evaporator section. This is due to the difference in density between the annulus and the downcomer.

A model describing both the thermal and phase flows of the closed two-phase double-tube thermosyphon (DTTH) has been performed. The theoretical model provides an accurate description of the behavior of our experimental setup based on experimental observations that show a simple exponential behavior. This simpler model has been developed, on the one hand, in order to provide numerical expressions of the variations in system variables and, on the other hand, to give the expression of the (DTTH) response time as a function of the various parameters. The initial basis of the model stems from the analysis previously conducted on test experiments, which suggests that the entire (DTTH) system can be viewed as a limited set of bodies that evolve linearly under the sole influence of thermal mechanisms. The first body represents the evaporator wall. It can be viewed as a thermally thin body, represented by a temperature (T_w). The second body corresponds to the entire working fluid, which interacts with both the evaporator wall and the working fluid. The working fluid was considered saturated and has a temperature (T_f). This model presents a theoretical investigation of the thermosyphon heat pipe behavior in a transient regime. The transient model was adopted to simulate the response of the thermosyphon. The transient thermal behavior of the thermosyphon has been utilized in order to obtain a mathematical expression of the system response. A computer simulation program based on the method was developed to estimate the temperature of the thermosyphon as well as the time needed to reach a steady state. This program can be considered a simple tool for modeling and designing a thermosyphon in a transient regime. The predictions of this model were found to be in general agreement with the experimental data.

Experimental setup

A research loop was built to examine the effect of heating rate, cooling rate, and heated length of the sub-cooled heat-pipe in real operation (warm-up, steady-state, and cool-down). The heat pipe is made of copper with a 0.32 cm internal diameter, a 0.15 cm thickness, and a 100 cm length. The evaporator section length is 0.6 m, the condenser section length is 0.25 m, and the adiabatic section length is 0.15 m. An inner tube composed of polypropylene is inserted inside the evaporator section

to form a hot channel between the inner and outer tubes, which increases the natural flow of liquid and creates sub-cooled liquid in the evaporator. Four electrical coils serve as the evaporator's heat source, while a cooling garment encircling the condenser section uses cooling water at room temperature and 0.06 MPa at constant pressure to

function as the heat sink. Also, the heat pipe test apparatus and the corresponding model modulization are illustrated in Figure (1). Along the heat-pipe, both the vapor and wall temperatures were recorded. In comparison to the theoretical model, the following heat pipe parameters were determined and assessed: The time constant and the heat transfer coefficients between the evaporator were dtermined and assessed.

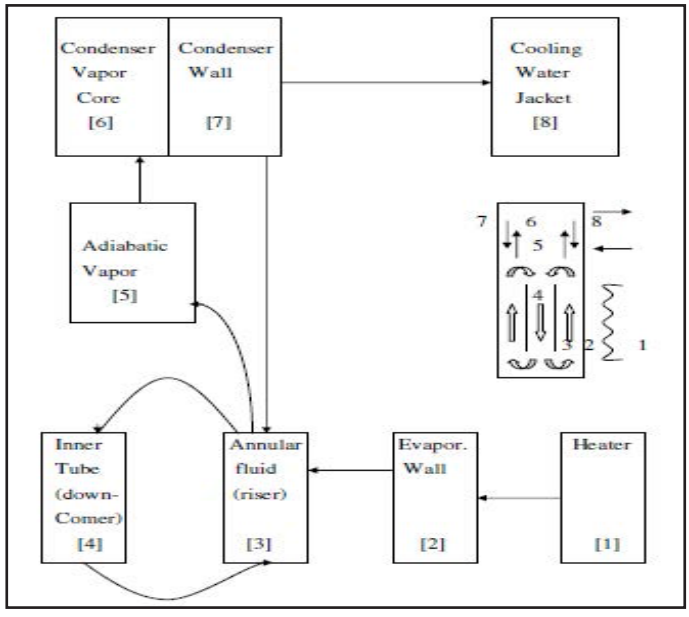

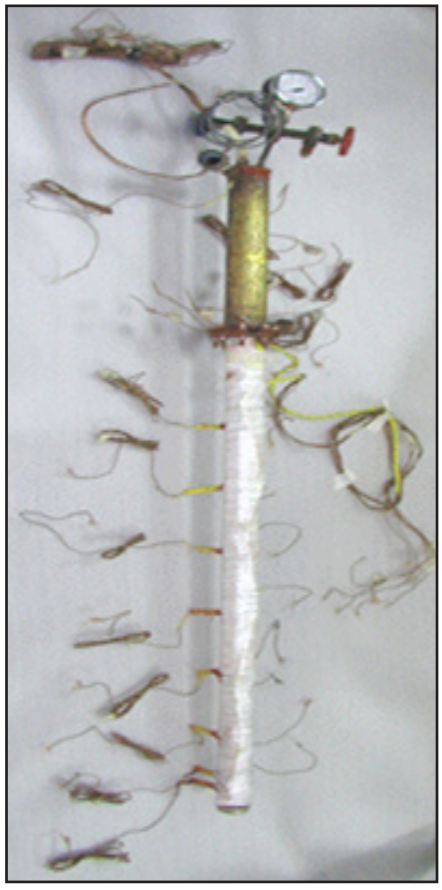

Figure (1): Loop Test rig, Model and its Corresponding Nodalization

The error in a measurement is usually defined as the difference between its true value and the measured value. The errors generated in experimental results are attributed to either manual errors, which are caused by the investigators, or instrumentation errors, which are due to the inaccuracy of measuring devices. Repeating the runs several times and taking the mean arithmetic value into consideration may minimize the first type of error. To determine the second type of error (instrumentation error), the sensitivity as a minimum readable value for each device must be represented. The accuracy of the measured and calculated parameters is shown in Table (1).

Table (1): Accuracy of measured and calculated parameters

No	Error	Parameter	Percentage error
1	measured	Heat load	10.71
2	Calculated	Cross sectional area	0.57
3	Measured	Temperature	2.85
4	Calculated	Overall heat transfer coefficient	14.13

Mathematical Model

The results from the mathematical model were based on the tested experiments. The heat-pipe is considered to be a collection of thermal mechanisms influenced by the body. The initial body denotes the evaporator wall, which is quantified in terms of temperature (T_w). The second substance, which possesses a temperature (T_f), was the entire working fluid that was deemed saturated. Thermal energy refers to a continuous flow of heat, while the cooling water was at the surrounding room temperature.

Data Reduction

The fluid and wall heat-balance equations are as follows:

$$C_w \frac{\partial T_w}{\partial t} = \dot{Q_e} - h_e S_e (T_w - T_f) \quad (1)$$

$$C_f \frac{\partial T_f}{\partial t} = h_e S_e (T_w - T_f) - h_c S_c (T_f - T_{wat}) \quad (2)$$

Where: S_e: the evaporator'sinner surface = $\pi^*D^*L_{evap.}$
S_c: the condenser'souter surface = $\pi^*D^*L_{cond.}$
C_f: working fluid'sthermal capacitance.
C_w: heat-pipe wall thermal capacitance.
T_w: wall temperature.
The evaporator wall temperatures change with time is expressed as:

$$\underbrace{\frac{d}{dt}\begin{pmatrix} T_w \\ T_f \end{pmatrix}}_{\dot{x}} = \underbrace{\begin{pmatrix} -\frac{h_c.S_c}{C_w} & \frac{h_c.S_c}{C_w} \\ \frac{h_e.S_c}{C_f} & \frac{h_e S_e + h_c S_c}{C_f} \end{pmatrix}}_{A} \begin{pmatrix} T_w \\ T_f \end{pmatrix} + \underbrace{\begin{pmatrix} \frac{\dot{Q_e}}{C_w} \\ \frac{T_{wat} h_c S_c}{C_f} \end{pmatrix}}_{\quad} \quad (3)$$

The analytical solution is obtained by the Farsi model using the linear algebraic formulation **(Farsi *et al.*, 2003)** as follows:

$$\vec{X}(t) = -A^{-1}\vec{X} + Me^{Dt}M^{-1}\left(\vec{X}_0 + A^{-1}\vec{B}\right) \quad (4)$$

The D matrix represents the diagonalized form of matrix A.

$$D = diag\left(-\lambda_{\max}, -\lambda_{\min}\right) \quad (5)$$

Where λ_{max} and λ_{min} are Eigenvalues and equation (5) can be written as:

$$e^{D} = \begin{pmatrix} e^{-(\lambda_{\max}t)} & 0 \\ 0 & e^{-(\lambda_{\min}t)} \end{pmatrix} \quad (6)$$

The matrix of eigenvectors is then represented as:

$$M = \begin{pmatrix} \alpha_w & \alpha_w \\ \lambda_w - \lambda_{\max} & \lambda_w - \lambda_{\max} \end{pmatrix} \quad (7)$$

By solving the equations, the formulas for T_w and T_f can be obtained as:

$$T_w(t) = T_{w,ss} + \frac{\dot{Q_e}}{C_w\left(\frac{1}{\tau_{min}} - \frac{1}{\tau_{max}}\right)}\left\{\left(\frac{1}{\lambda_w} + \frac{C_w}{C_f(\lambda_f - \alpha_f)}\right)\left(\frac{1}{\tau_{max}}e^{-(t/\tau_{min})} - \frac{1}{\tau_{min}}e^{-(t/\tau_{max})}\right)\right\} - \left(e^{-(t/\tau_{min})} - e^{-(t/\tau_{max})}\right) + \frac{T_{w,0} - T_{wat}}{\frac{1}{\tau_{min}} - \frac{1}{\tau_{max}}}\left\{\left(\frac{1}{\tau_{min}} - \lambda_f\right)e^{-(t/\tau_{min})} - \left(\frac{1}{\tau_{max}} - \lambda_f\right)e^{-(t/\tau_{min})}\right\} - \frac{T_{f,0} - T_{wat}}{\frac{1}{\lambda_w}\left(\frac{1}{\tau_{min}} - \frac{1}{\tau_{max}}\right)}\left(e^{-(t/\tau_{min})} - e^{-(t/\tau_{max})}\right) \quad (8)$$

$$T_f(t) = T_{f,ss} + \frac{\dot{Q}}{C_w\left(\frac{1}{\tau_{min}} - \frac{1}{\tau_{max}}\right)}\left\{\left(\frac{C_w}{C_f(\lambda_f - \alpha_f)}\right)\frac{1}{\tau_{max}}\left(e^{-\left(\frac{t}{\tau_{min}}\right)} - e^{-\left(\frac{t}{\tau_{max}}\right)}\right)\right\} - \frac{T_{w,0} - T_{wat}}{\frac{1}{\alpha_f}\left(\frac{1}{\tau_{min}} - \frac{1}{\tau_{max}}\right)}\left(e^{-(t/\tau_{min})} - e^{-(t/\tau_{max})}\right) + \frac{T_{f,0} - T_{wat}}{\frac{1}{\tau_{min}} - \frac{1}{\tau_{max}}}\left\{\left(\frac{1}{\tau_{min}} - \lambda_w\right)e^{-(t/\tau_{min})} - \left(\frac{1}{\tau_{max}} - \lambda_w\right)e^{-(t/\tau_{max})}\right\} \quad (9)$$

Where τ_{min} and τ_{max} represent time, constants associated with the sub-cooled heat-pipe's response.

$$\alpha_w = \lambda_w = \frac{h_e S_e}{C_w},\ \alpha_f = \frac{h_e S_e}{C_f},\ \lambda_f = \frac{h_e S_e + h_c S_c}{C_f}$$

$$T_{w,ss} = T_{wat} + \frac{\dot{Q_e}}{C_w}\left(\frac{1}{\lambda_w} + \frac{C_w}{C_f(\lambda_f - \alpha_f)}\right) \quad (10)$$

$$T_{f,ss} = T_{wat} + \frac{\dot{Q_e}}{C_w}\left(\frac{C_w}{C_f(\lambda_f - \alpha_f)}\right) \quad (11)$$

The resolution of these equations yields the subsequent mathematical expressions:

$$\lambda_{max} = \frac{\lambda_w + \lambda_f}{2} + \sqrt{\left(\frac{\lambda_w - \lambda_f}{2}\right)^2 + \alpha_w\alpha_f} = \frac{1}{\tau_{min}} \quad (12)$$

$$\lambda_{min} = \frac{\lambda_w + \lambda_f}{2} - \sqrt{\left(\frac{\lambda_w - \lambda_f}{2}\right)^2 + \alpha_w\alpha_f} = \frac{1}{\tau_{max}} \quad (13)$$

Actual load, $\dot{Q}_{net}$

The heat load refers to the amount of heat that is extracted from the condenser cooling jacket.

$$\dot{Q}_{net} = [\dot{m} * C_p (T_o - T_i)]_{cw} \quad (14)$$

$$\dot{Q}_{net} = [h_e * S_e (T_w - T_f)] \quad (15)$$

Where $\dot{m}_{cw}$ is the water mass flow rate and, $C_{p,cw}$ is the average specific heat of water in the jacket and evaluated at average water temperature $(T_o - T_i)_{cw}/2$.

The evaporator Heat flux, q_r

Radial heat flux, $q_r = Q_{net}/A_r = Q_{net}/(\pi * d_i * L_e)$ (16)

The sub-cooled heat-pipe axial heat flux is

$$q_{ax} = Q_{net}/A_{c.s} = Q_{net}/(\pi * d_i^2/4) \quad (17)$$

Average evaporator heat transfer coefficient, h_e

The flow boiling in the sub-cooled thermosyphon is propelled by the natural circulation, which is induced by the density difference between the annulus and the downcomer. By means of empirical correlation, the calculation of the heat transfer coefficient in two-phase flow has performed. The coefficient heat transfer of two-phase correlation is proposed by **Whalley (1989)**:

$$h_e = \frac{0.00122 \cdot \Delta T_{sat}^{0.24} \cdot \Delta P_{sat}^{0.75} \cdot cp_l^{0.45} \cdot \rho^{0.49} \cdot k_l^{0.79}}{\sigma^{0.5} \cdot h_{fg}^{0.24} \cdot \mu_L^{0.29} \cdot \rho_g^{0.24}} \quad (18)$$

Average coefficient heat-transfer of the cooling section, hc

The average cooling water coefficient heat transfer (h_c) can be calculated as:

$$h_c = 1.86 \cdot (Re_{cw} \cdot Pr_{cw})^{0.33} \cdot \left[\frac{d_{h,cw}}{L_c}\right]^{0.33} \cdot \frac{K_{cw}}{d_{h,cw}} \quad (19)$$

The Over-all heat transfer coefficient, U

The sub-cooled heat pipe transfers heat from the source to the sink in the manner of a technical single conductor. The overall heat transfer coefficient is often determined using the following equation.

$$U = \frac{q_{ax.}}{(T_w - T_{cond})} \quad (20)$$

Effective thermal conductivity

The thermal conductivity, denoted as K_{eff}, is the result of heat transfer occurring during the liquid-vapor phase change, which the evaporator transfers the heat to the

condenser. The given statement describes the correlation among the power input and the thermal conductivity of a sub-cooled heat pipe.

$$K_{eff} = U * L_{eff} \quad (21)$$

Results and Discussions

Average Wall Temperature

The theoretical and experimental results of the sub-cooled heat pipe's average outer surface temperature are shown in Figures (2-5). The results are different depending on how the pipe is used. The findings indicate that experimental measurements and theoretical results are comparatively congruent. The mean wall temperature was measured at various time increments, considering the input power, water flow rates, and evaporator lengths. Throughout the cycle, a minor deviation of 2% to 8% is detected. The mean wall temperature of the experiment has some deviation that may be attributed to the vacuum level due to vacuum pump capability. Regarding the experimental system in question, it is believed that the numerical model represents an ideal situation.

Cooling Water Flow Effects

The impact of cooling water flow rate on the transient response is examined under the evaporator length, power of heating, and annulus width. of the sub-cooled heat pipe is investigated in small increments ranging from 20 g/s to 90 g/s. Figure (2) depicts the average evaporator outer wall temperature for a sub-cooled heat pipe at various cooling rates, representing the warm-up and cool-down of the prototypical system under steady state conditions. Figure (3) shows the test results for warm-up and cool-down of the average evaporator outer wall temperature under steady state for a sub-cooled heat pipe with different cooling rates under identical conditions. 1000 W of thermal power is constant. Increased cooling water discharge from 20 g/s to 90 g/s lowered the wall temperature under steady state from 64.7 to 54.6 °C. An elevated convective heat transmission coefficient results in a reduction in the average cooling water temperature of the garment. The sub-cooled thermosyphon's steady-state wall temperature decreases with a reduced water temperature. The condenser temperature rises as the average water temperature in the cooling jacket lowers.

Effect of Input Power

The study investigates the impact of heating power on the dynamic behavior of the sub-cooled pipe by adjusting the power provided to the heater in the evaporator. The cooling garment ensures that the cooling water discharge rate stays constant at 40 g/s. The power supplied to the heater is increasing by 100 W increments, from 0.9 kW to 1.6 kW. Figure (4) illustrates the impact of heat load on the wall temperature, while maintaining a similar cooler flow rate. The findings suggest that an increase in heating capacity leads to a concomitant rise in both the initial rates of heat up and smooth values of wall temperature at normal steady-state conditions. The experimental steady-state wall temperature rose from 57.1 to 78 °C, while the theoretical wall temperature in steady-state rose from 57 to 74 °C as the electric power was increased from 0.9 kW to 1.6 kW.

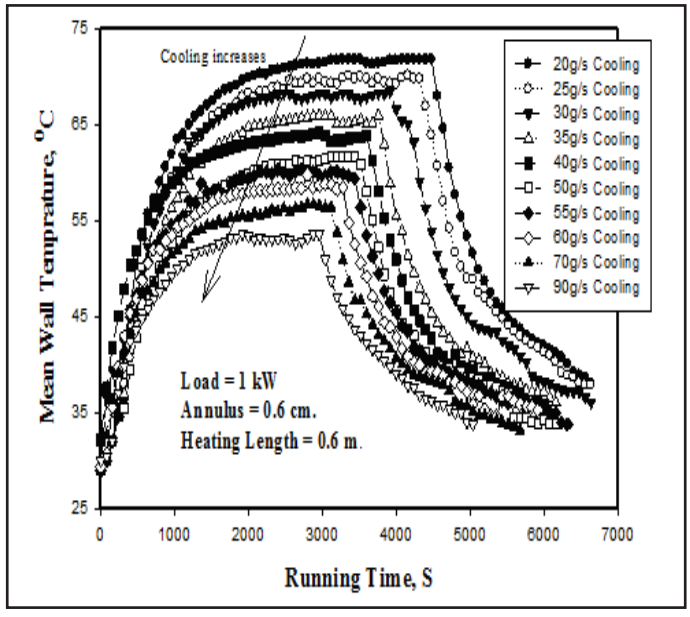

Figure (2): Theoretical worm-up, stable-state and cool-down of mean evaporator wall temperature for sub-cooled heat-pipe at variable cooling rate.

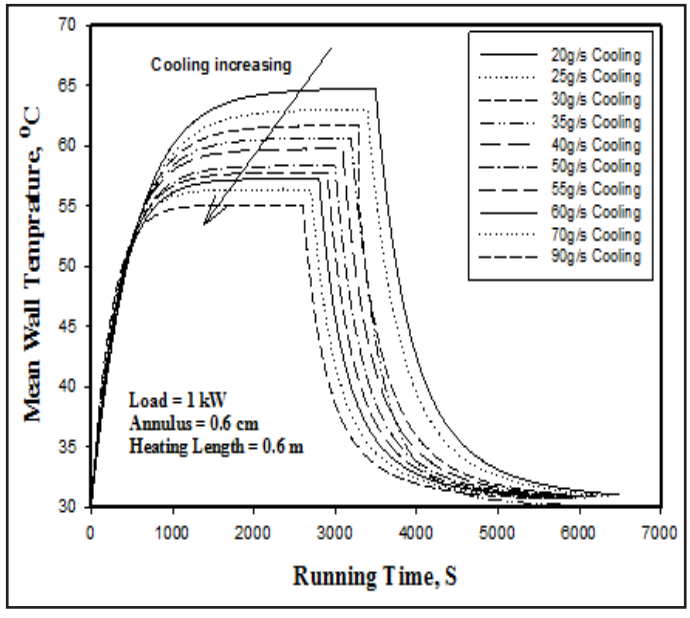

Figure (3): Experimental worm-up, stable-state and cooldown of mean evaporator wall temperature for subcooled heat-pipe at variable cooling rate.

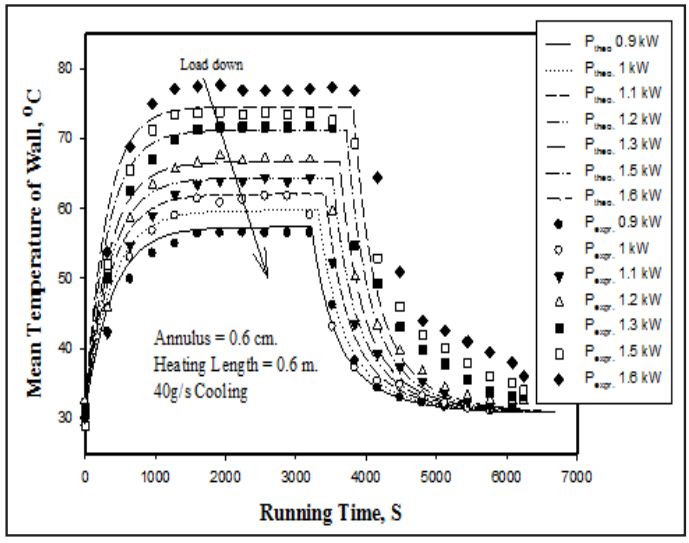

Figure (4): Theoretical and experimental worm-up, stable-state and cool-down of mean evaporator wall temperature for subcooled heat-pipe at variable heat-loads.

Effect of Evaporator Length

At a constant flow rate of 40 g/s of cooling water in the cooling sleeve at the condenser jacket, the evaporator length of the sub-cooled heat pipe has a significant influence on the mean wall temperature. At a 4 mm annulus width and 1 kW heating capacity, the evaporator lengths are dictated by the sub-cooled heat pipe's transient response. Figure (5) shows the experimental and theoretical average evaporator outer wall temperature for a sub-cooled heat pipe at various lengths as warm-up, and cool-down. The average temperature of the wall rises as the evaporator length increases. Experimental and theoretical results correspond well for 0.6 m, 0.45 m, and 0.3 m evaporators. At the 15 cm evaporator length, disagreement arises when the system approaches the sub-cooled heat-pipe limit due to increased heat flux.

Average Fluid Temperature

Developing and designing a theoretical model to simulate the operating parameters of a sub-cooled thermosyphon. The transient behavior of the annulus fluid, two phases, and inner tube vapor, one phase, are emulated, as well as the adiabatic and condenser sections. It is also possible to predict the temperature behavior of the sub-cooled thermosyphon, from warm-up to steady-state and even cool-down. Experimentation is conducted to clear the sub-cooled heat-pipe at the same average fluid temperature from initialization to steady-state to deceleration under a variety of operating parameters. As the cooling water flow rate diminishes, the mean temperature of the working fluid within the sub-cooled heat-pipe causes it to rise gradually, which ranges from 20 to 90 g/s at a thermal load of 1 kW and an evaporator length of 60 cm. The theoretical and experimental mean fluid temperatures for a sub-cooled heat pipe at various cooling flow rates are depicted in Figures (6) and (7), respectively. As a result of the reduced cooling flow rate over time, temperatures increase substantially at the onset of operation. The rate at which the system attains a stable state is inversely proportional to the difference in temperature. The steady state fluid temperature at the sub-cooled thermosyphon was determined to be between 47.2 and 57.8 °C, which is consistent with the experimental findings. The electric power that simulates the transported heat is a critical operating parameter of sub-cooled heat pipes; it was altered between 0.9-1-1.1-1.2-1.3-1.5 kW and 1.6 kW. The theoretical and experimental mean fluid temperatures for a sub-cooled heat-pipe under varying heating loads are depicted in Figure (8). Once the heat transfers to the wall, the liquid is heated. After the liquid undergoes evaporation, the vapor ascends towards the condenser section for a second freezing process. The results suggest 3–6% concordance data. Figure (9) shows the experimental and theoretical average fluid temperature for a sub-cooled heat-pipe at different evaporator lengths. Variations in evaporator length, accompanied by a consistent water-cooling flow rate of 40 g/s and a constant heat burden of 1 kW, result in a progressive increase in fluid temperature over time due to the accelerated heat rate. Consistent with experimental findings, the average fluid temperature remains constant within the evaporator length range of 0.6 m to 0.45 m. A 0.3 m evaporator length yields good agreement. The high heat flow nearing the sub-cooled heat pipe's limit may explain the lower agreement than the 0.15 m evaporator length.

Various operating parameters' net power output from the condenser of the sub-cooled heat pipe over time is illustrated in Figures (10) and (11). The heater transfers thermal energy to the wall, and the wall subsequently transfers the heat to the fluid. Both processes exhibit an increase over time. The gradual decline in heat absorption within each segment can be attributed to the augmented thermal diffusivity of the fluid, wall, and heater. Heat losses from the sub-cooled heat pipe and heat transported by the sub-cooled heat pipe transfer heat through conduction, convection, insulation, and radiation. When it is in a steady state, the electric system generates this heat. Over time, the rate of heat emission during shutdown gradually diminishes until it reaches zero. By conniving the heat exclusion in the condenser cooling sleeve using equation [11], the heat load is calculated. Theoretical and experimental output heat rates under varying heat loads while maintaining a constant cooling flow rate and evaporator length are depicted in Figure (12). Theoretical and experimental outcomes for varying evaporator lengths under constant heat load and chilling rate conditions are depicted in Figure (13). The thermal losses in the experimental measurements contributed to a lesser

degree, as indicated by the figures. From its initial state, power application initiates the heat transference through the sub-cooled thermosyphon. A portion of the heat that is transferred to the wall is absorbed internally by the wall, leading to a rise in temperature. The fluid then undergoes this thermal transfer. As heat transfers from the fluid's wall to it, its temperature progressively rises. As a result of the latent heat of evaporation, when heat is introduced to a fluid at its saturation temperature, the saturated fluid begins to evaporate. Following this, the heat rate is transferred from the condenser to the evaporator, where it is discharged into the thermal reservoir. In actuality, the heat extracted is the heat transported along the sub-cooled heat-pipe.

Theoretical and experimental results show good agreement at evaporator lengths of 60, 45, and 30 cm, but at an evaporator length of 15 cm, there is some disagreement. This may be due to higher heat flux, which makes it closer to the vicinity of the thermosyphon limit.

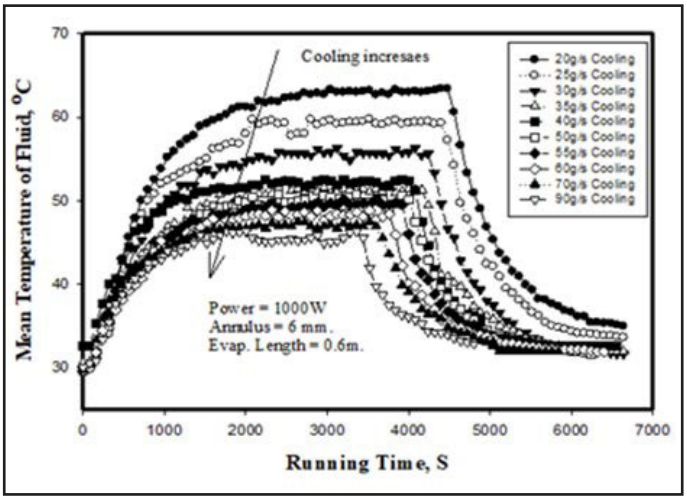

Figure (7) Experimental warm-up, stable-state and cool-down of mean fluid temperature for sub-cooled heat-pipe at variable cooling rate.

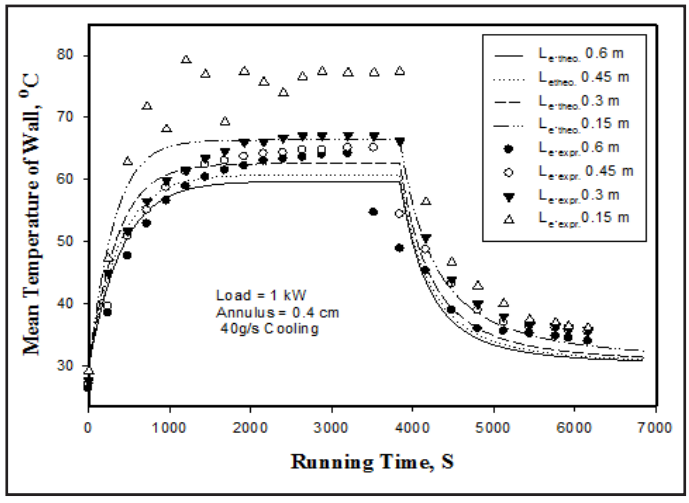

Figure (5): Experimental and theoretical worm-up, stablestate and cool-down of mean evaporator wall te per ture for sub-cooled heat-pipe at variable evaporator lengths.

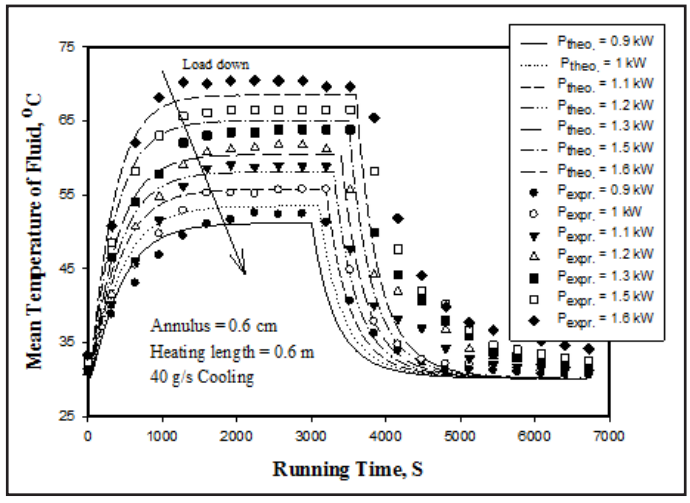

Figure (8): Investigate warm-up, and cool-down under stable state of mean fluid temperature for subcooled heat-pipe at variable loads of heating.

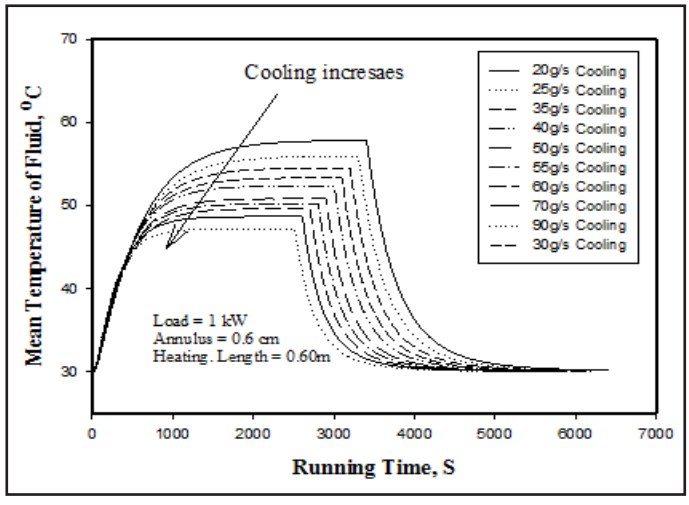

Figure (6): Theoretical warm-up, stable-state and cool-down of mean fluid temperature for sub-cooled heat-pipe at variable cooling rate.

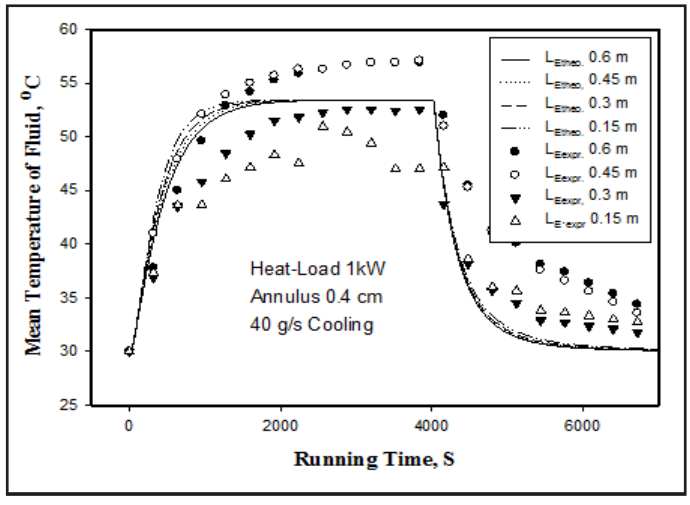

Figure (9): Experimental and theoretical warm-up, stablestate and cool-down of mean fluid temperature for sub-cooled heat-pipe at variable evaporator-lengths.

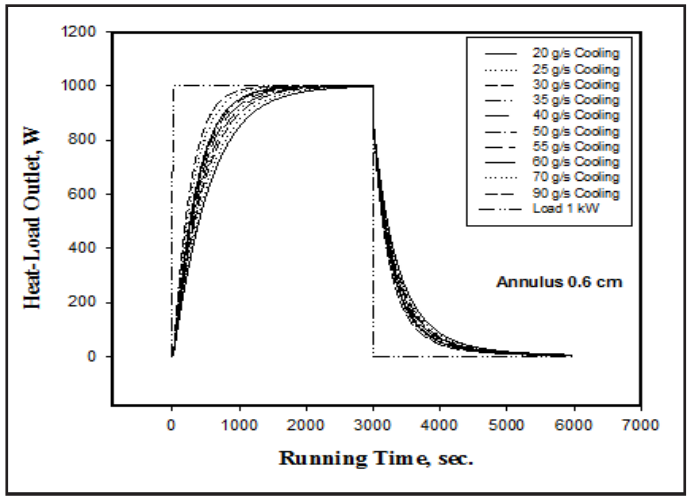

Figure (10): Theoretical power output for sub-cooled heat-pipe during warm-up, stable-state and cool-down at annulus 6mm and Power 1 kW variable coolant-rates.

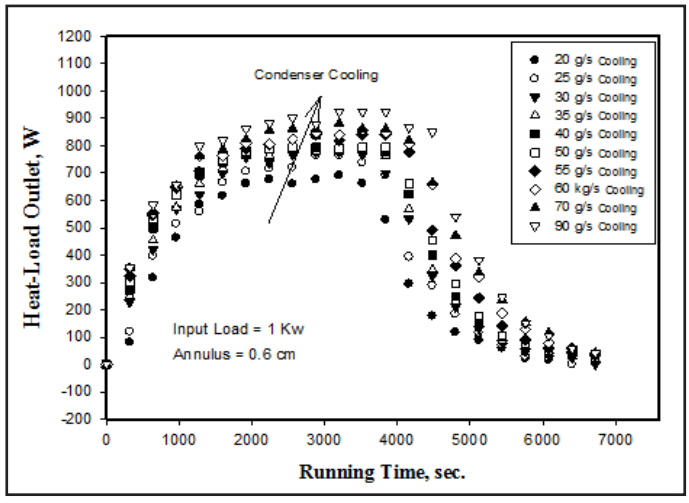

Figure (11): Experimental power output for sub-cooled heat-pipe during warm-up, stable-state and cool-down at variable coolant-rates.

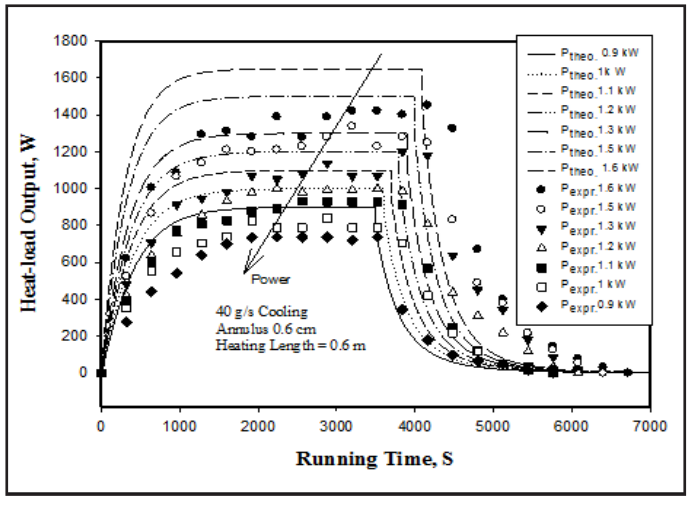

Figure (12): Experimental power output for sub-cooled heat-pipe during warm-up, stable-state and cool down at variable power in-put.

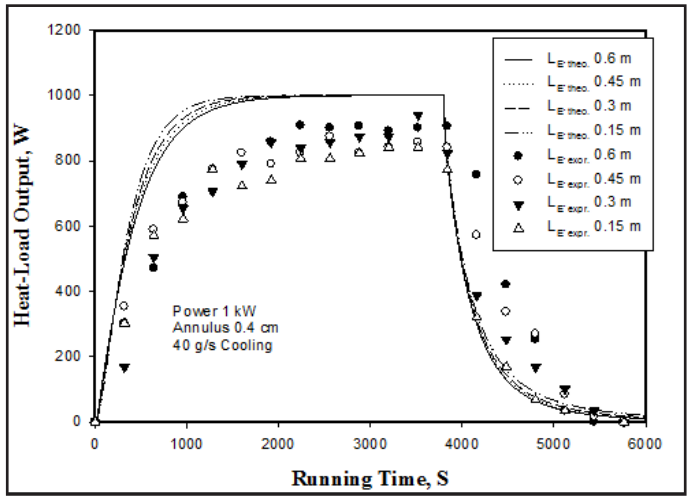

Figure (13): Experimental power output for subcooled heat-pipe during warm-up, stable-state and cool-down at variable evaporator lengths.

Conclusions

The mathematical model findings of the sub-cooled heat-pipe are derived from the conducted experiments. The creation of a computer simulation designed to predict all aspects of dynamic functioning. Multiple metrics are measured, including the thermal conductivity, the time needed to achieve a stable condition, the average temperature of the heat pipe on the wall, the output power, and the total coefficient of heat transfer. The program is widely regarded as an effective tool for modeling and simulating the heat-pipe in warm-up, steady-state, and cool-down conditions. The measured values for the average wall temperature, fluid temperature, and power dissipated show a strong agreement with the theoretically expected statistics. The results demonstrate a 3% to 6% agreement between the theoretical model and the experimental data. The discrepancy between the theoretical and practical results can be attributed to the dissipation of heat in the experimental experiments. The evaporator length of the sub-cooled heat pipe has a significant impact on the power output and mean wall temperature in the condenser cooling jacket when the cooling flow rate of water is kept constant.

Nomenclature

d: inside diameter (m)
e: wall thickness (m)
h: heat transfer coefficient ($W/m^2 K$)
P: pressure (Pa)
q: flux's heat ($W\ m^2$)
Q: rate of heat transfer (W)
S: surface area (m^2)
T: temperature (°C)
t: time (s)

X: $T_{w,}$ T_f, and P
ΔT: liquid superheated (°C)

Greek letters
γ: heat-pipe filling ratio (%)
ρ: density(kg/m^3)
τ: time constant (s)

Subscripts
c: condenser
e: evaporator
f: working fluid
l: liquid
o: initial value
ss: steady state
v: vapor
w: wall
wat: water

Dimensionless Groups
Pr: Prandtl number (C_pm/k),
Re: Reynolds number (4qL/h)

References

- **Chen, Y.; Groll, M.; Mertz, R.; Maydanik, Y.F. and Vershininb, S.V. (2006):** Steady-state and transient performance of a miniature loop heat pipe. *Int. J. Therm. Sci*., 45: 1084.
- **Chen, X.; Ye, H.; Fan, X.; Ren, T. and Zhang, G. (2016):** A review of small heat pipes for electronics. *Appl. Therm. Eng*., 96: 1-17.
- **Dobson, R.T. and Ruppersberg, J.C. (2007):** "Flow and heat transfer in a closed loop thermosyphon. Part II – theoretical simulation. *J. Ener. South. Af*., 18: 41.
- **Dobson, R.T. and Ruppersberg, J.C. (2007):** Flow and heat transfer in a closed loop thermosyphon. Part I – theoretical simulation", *Journal of Energy in Southern Africa*., 18: 32 – 40.
- **El-Genk, M.S. and Huang, L. (1993):** An experimental investigation of the transient response of a water heat pipe. *Int. J. Heat Mass Transf*., 36: 3823.
- **Farsi, H.; Joly, J.; Miscevic, M.; Platel, V. and Mazet, N. (2003):** An experimental and theoretical investigation of the transient behavior of a two-phase closed thermosyphon. *Appl. Ther. Eng*., 23: 1895.
- **Harley, C. and Faghri, A. (1994):** Complete transient two-dimensional analysis of two-phase closed thermosyphons including the falling condensate film. *J. Heat Trans. Trans. ASME*., 116: 418.
- **Hua, Z.; Jian-xin, W.; Qiao-hui, Z. and Chuan-jing, T. (2004):** Experimental study on transient behavior of semi-open two-phase thermosyphon. *J. Zhejiang Univ. Sci*., 5(12): 1565.
- **Huang, L; Elgenk, M.S. and Tournier, J. (1993):** Transient performance of an inclined water heat pipe with a screen wick. Heat Pipes and Capillary Pumped Loops, *ASME Heat Transfer Division*., 236: 87-92.
- **Hussein, H.M.S. (2002):** Optimization of a natural circulation two phases closed thermosyphon flat plate solar water heater. *Energy Conversion and Management*., 44: 2341-2352.
- **Imura, H.; Koito, Y.; Mochizuki, M. and Fujimura, H. (2005):** Start-up from the frozen state of two-phase thermosyphons. *App. Therm. Eng*., 25: 2730.
- **Ji, Y.; Yuan, D.; Hao, Y.; Tian, Z.; Lou, J. and Yunyun W. (2020):** Experimental study on heat transfer performance of high temperature heat pipe with large length-diameter ratio for heat utilization of concentrated solar energy. *Appl. Therm. Eng.,* 215: 118918.
- **Kamel; Shamloul, M.; Sadaawy, M. and Zoklot, A. (2006):** Thermal Characteristics of The Closed Two-phase Thermosyphon with Inner Tube. M.Sc. thesis, Zagazig University.
- **Kang, Z.; Hong, Y.; Jiang, S. and Fan, J. (2023):** Composite filament with super high effective thermal conductivity, *Mater. Today Phys*., 34: 101067.
- **Kwon, C. H.; Kwon, H.S.; Oh, H.U. and Jung, E. G. (2023):** "Experimental investigation on acceleration of working fluid of heat pipe under bypass line operation. *Case Study Thermal. Eng*., 53: 103742.
- **Legierski, J.; Wie_cek, B. and Mey, Gi. (2006):** Measurements and simulations of transient characteristics of heat pipes. *Microelectr. Reliab*., 46: 109.
- **Li, Y.; Li, N.; Shao, B.; Dong, D. and Jiang, Z. (2023):** Theoretical and experimental investigations on the supercritical startup of a cryogenic axially Ω-shaped grooved heat pipe. *Appl. Therm. Eng*., 222: 119951.
- **Li, Z.; Zhang, H.; Huang, Z.; Zhang, D. and Wang, H. (2022):** Characteristics and optimization of heat pipe radiator for space nuclear propulsion spacecraft, *Prog. Nucl. Energy*., 150: 104307.
- **Lin, L. and Faghri, A. (1998):** An analysis of two-phase flow stability in a thermosyphon with tube separator. *Appl. Therm. Eng*., 18: 441.
- **Liu, J.; Yu, D.; Chen, G.; Shah, S.; Li, T. and Pan, C. (2023):** Numerical analysis of transient heat and mass transfer for a water heat pipe under non-uniform heating conditions. *Ann. Nucl. Energy*., 193.
- **Parand, R.; Rashidian, B.; Ataei, A. and Shakiby, Kh.; (2009):** Modeling the Transient Response of the Thermosyphon Heat Pipe. *J. Appl. Sci*., 9: 1531.
- **Patel, V.K. (2018):** An efficient optimization and comparative analysis of ammonia and methanol heat pipe for satellite application, *Energy Convers. Manag*., 165: 382–395.
- **Ramos, J.I. and Dobran, F. (1986):** Stability analysis of a closed thermosyphon model. *Appl. Math Mod.*, 10: 61.
- **Reed, J.G. and Tien, C.L. (1987):** Modeling of the two-phase closed thermosyphon. *J. Heat Trans*., 109: 722.
- **Saadawy, M.S.; Abo El-Nasr, M.M. and Abd El-Aziz, M. (2004):** Feasibility of The New Type- The Closed Two-Phase

Double Tube Thermosyphon (CTP- DTT): Performance Study. *Sci. Bull. Fac. Eng. Ain Shams Univ*., 39(3): 923.

- **Saadawy, M.S.; Abo El-Nasr, M.M. and Abd El-Aziz, M. (2004):** Investigation of boiling Heat Transfer Characteristics of Double-Tube Thermosyphon (DTT). 13th *Int. Heat Pipe Conf. Shangai, Chaina*., September 21-25: 333.
- **Silverstein, C.C. (1992):** Design and Technology of Heat Pipes for Cooling and Heat Exchange. Hemisphere Publishing Corporation, Washington (U.S.A.). https://doi.org/10.1201/9780367813598
- **Tian, Z.; Liu, X.; Wang, C.; Zhang, D.; Tian, W.; Qiu, S. and Su, G.H. (2021):** Experimental investigation on the heat transfer performance of high-temperature potassium heat pipe for nuclear reactor. *Nuc. Eng. Des*., 378: 111182.
- **Wang, G.S.; Song, B. and Liu, Z.H. (2010):** Operation characteristics of cylindrical miniature grooved heat pipe using aqueous CuO nanofluids. *Exp. Therm Fluid Sci*., 34: 1415.
- **Wang, Y. and Vafai, K. (2000):** Transient characterization of flat plate heat pipes during startup and shutdown operations. *Int. J. Heat Mass Trans*., 43: 2641.
- **Weragoda, D.M.; Tian, G.; Burkitbayev, A.; Lo, K.H. and Zhang, T.A. (2023):** Comprehensive review on heat pipe-based battery thermal management systems. *Appl. Therm. Eng*., 18: 120070.
- **Whalley, P.B. (1989):** Boiling Condensation and Gas-Liquid Flow. Department of Engineering Science. University of Oxford: p. 124-135.
- **Zeghari, K.; Louahlia, H.; Tiffonnet, A.L. and Schaetzel, P. (2023):** Micro-grooved circular miniature heat pipe for thermal management: Experimental and analytical investigations. *Therm. Sci. Eng. Progress*., 40: 101714.
- **Zhang, Z.; Chai, X.; Wang, C.; Sun, H.; Zhang, D.; Tian, W.; Qiu, S. and Su, G.H. (2021):** Numerical investigation on startup characteristics of high temperature heat pipe for nuclear reactor. *Nuc. Eng. Des*., 378: 111180.
- **Zhanga, C.; Chen, Y.; Shi, M. and Peterson, G.P. (2009):** Optimization of heat pipe with axial "Ω"-shaped micro grooves based on a niched Pareto genetic algorithm (NPGA). *Appl. Therm. Eng*., 29: 3340.
- **Zuo, Z. J. and Faghri, A. (1998):** A network thermodynamic analysis of the heat Pipe *Int. J. Heat Mass Trans*., 41: 1473.